Supporting Information for

Measurement report: Variability in ambient BVOC compositions along a latitudinal transect of Chinese forests

Di Liu[1], Jianqiang Zeng[2], Hua Fang[2,a], Zhenfeng Wu[2], Shaoxuan Xiao[2], Junjun Deng[3], Pingqing Fu[3], Yanli Zhang[2,4], Ping'an Peng[2], Xinming Wang[2,4,*]

[1]School of Environment, Beijing Normal University, Beijing 100875, China

[2]State Key Laboratory of Advanced Environmental Technology and Guangdong Key Laboratory of Environmental Protection and Resources Utilization, Guangzhou Institute of Geochemistry, Chinese Academy of Sciences, Guangzhou 510640, China

[3]Institute of Surface-Earth System Science, School of Earth System Science, Tianjin University, Tianjin, 300072, China

[4]College of Resources and Environment, University of Chinese Academy of Sciences, Beijing 100049, China

Correspondence to: Yanli Zhang (zhang_yl86@gig.ac.cn) and Xinming Wang (wangxm@gig.ac.cn)

[a]Now at School of Ecology and Environment, Anhui Normal University, Wuhu 241000, China

Contents of this file

Figures S1 to S16
Tables S1 to S6

Introduction

This supporting information is shown to support the scientific conclusions in the manuscript.

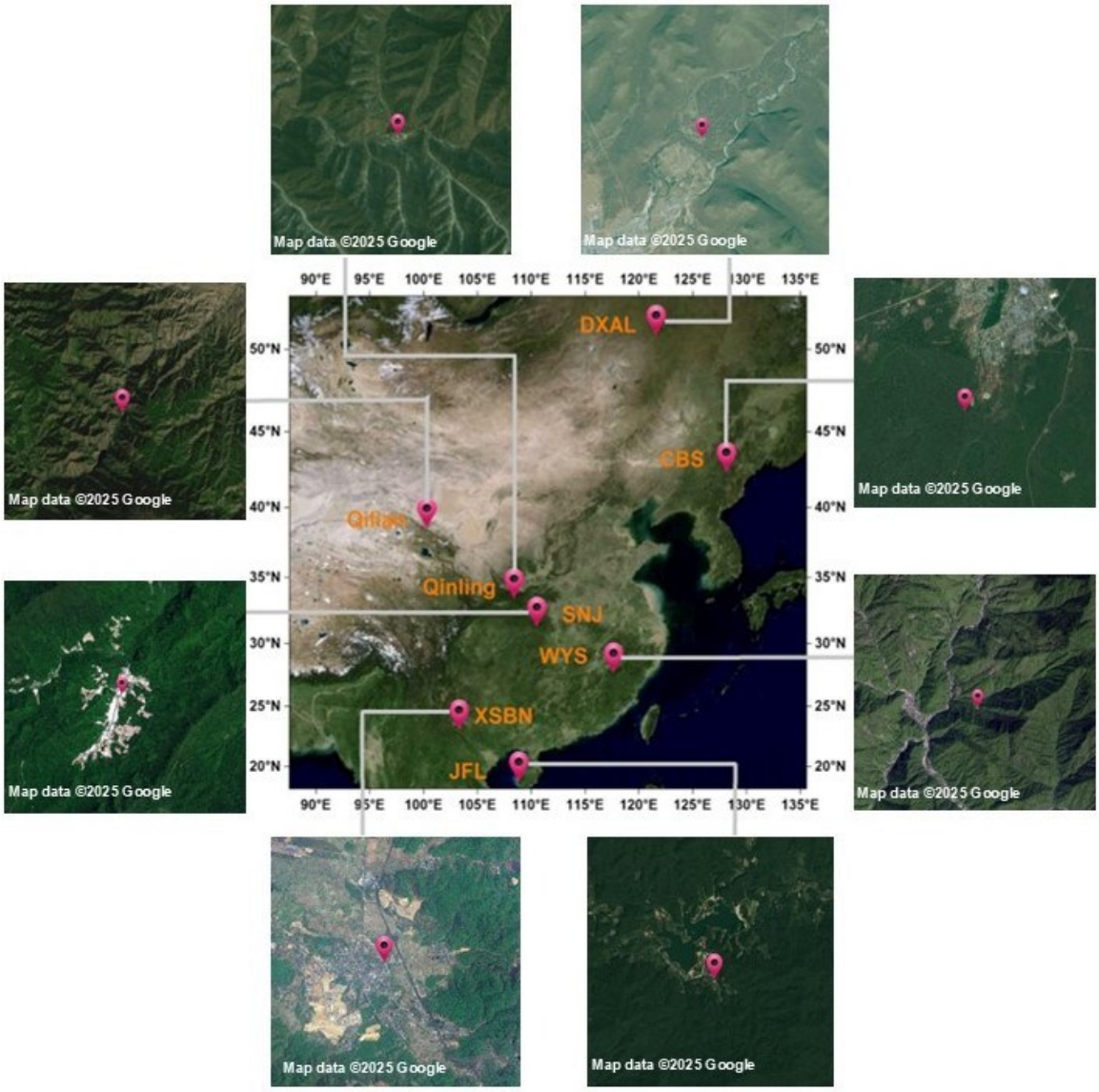


Figure S1. Measurement sites of this study. The base map is available at https://earth.google.com.

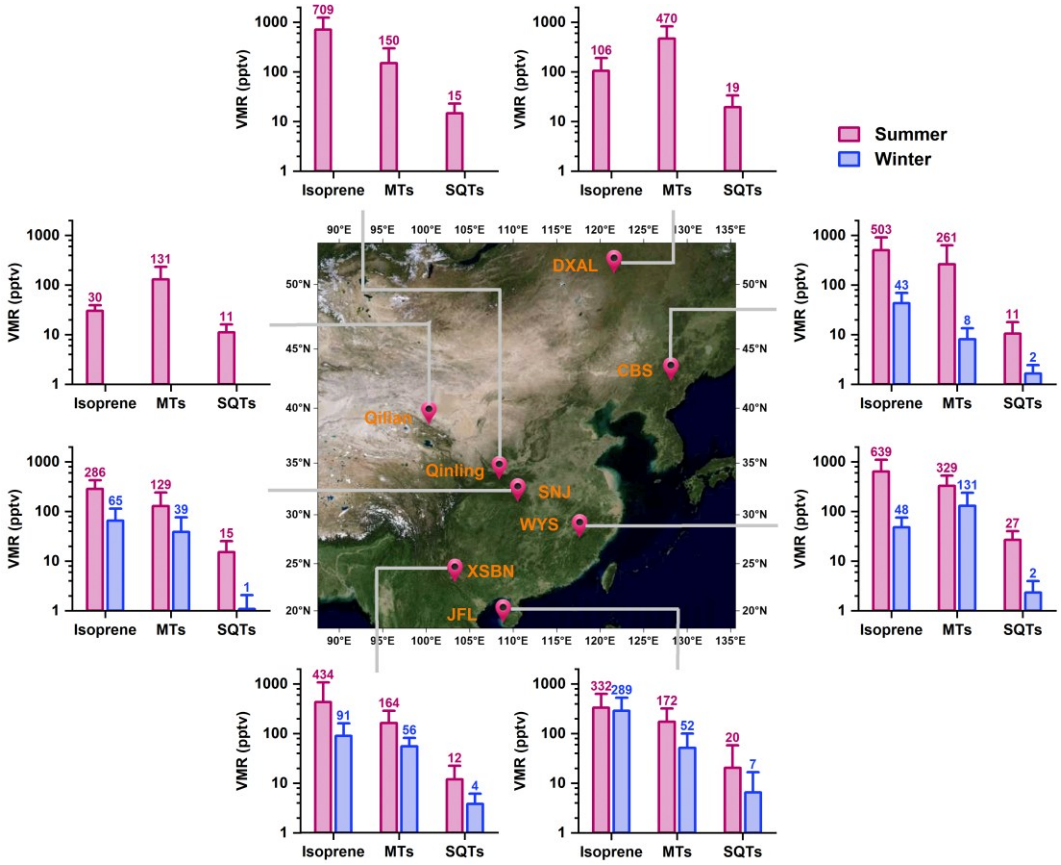


Figure S2. Mean BVOC mixing ratios at different forest sites in summer and winter.

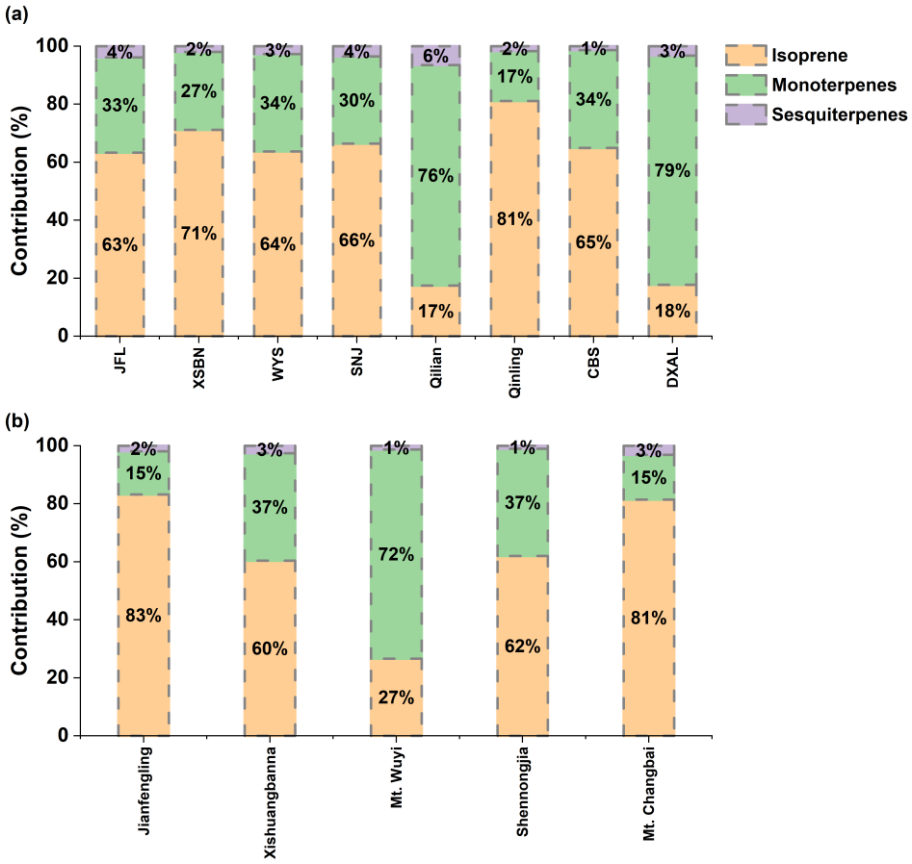


Figure S3. Composition of BVOCs in summer (a) and winter (b).

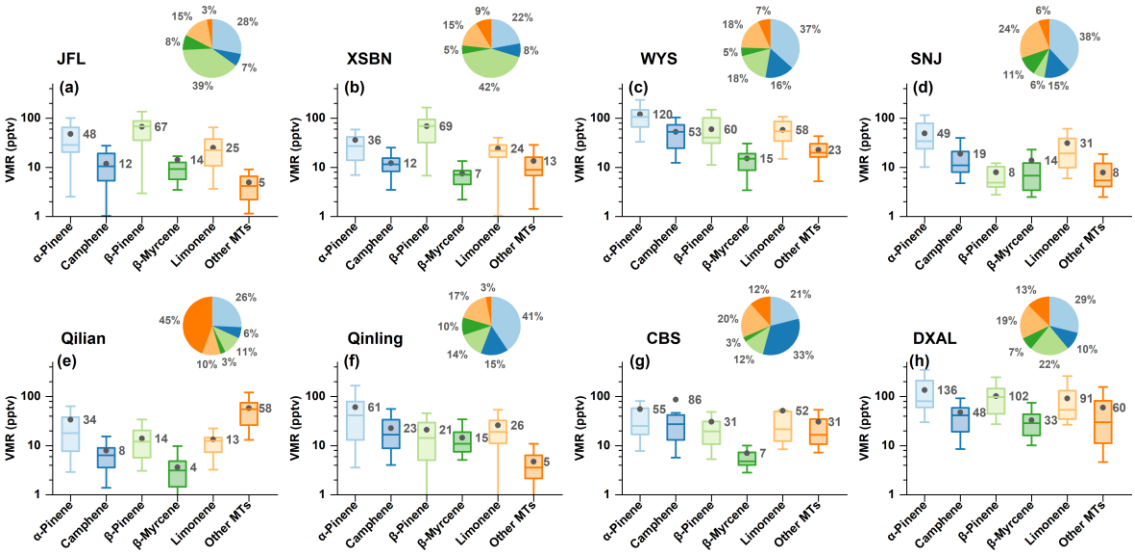


Figure S4. Mixing ratios and compositions of speciated MTs in summer.

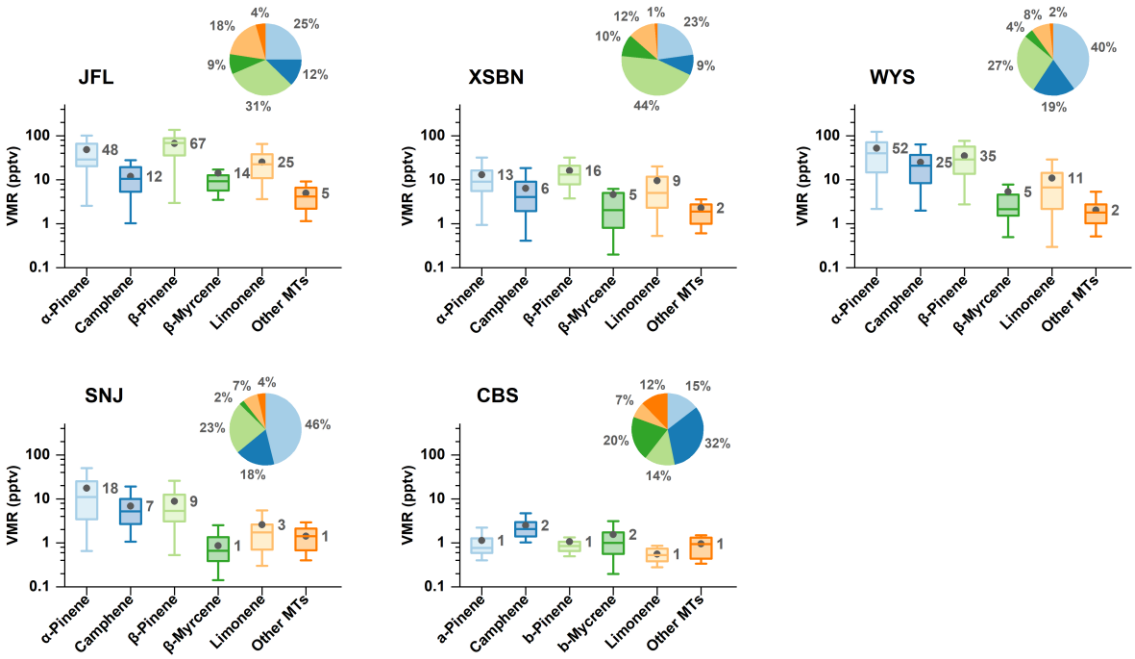


Figure S5. Mixing ratios and compositions of speciated MTs in winter.

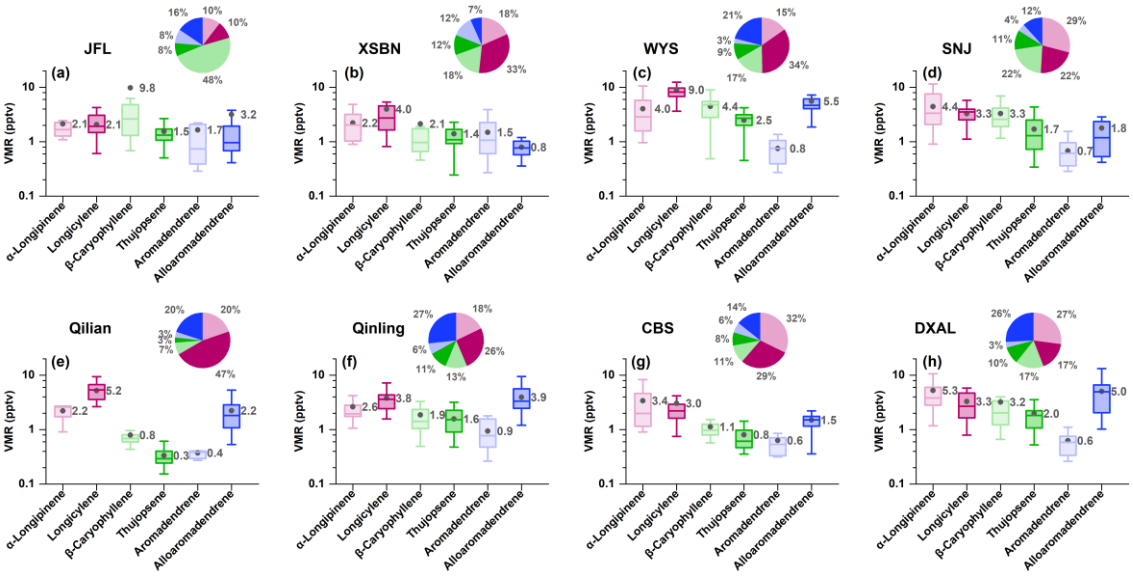


Figure S6. Mixing ratios and compositions of speciated SQTs in summer.

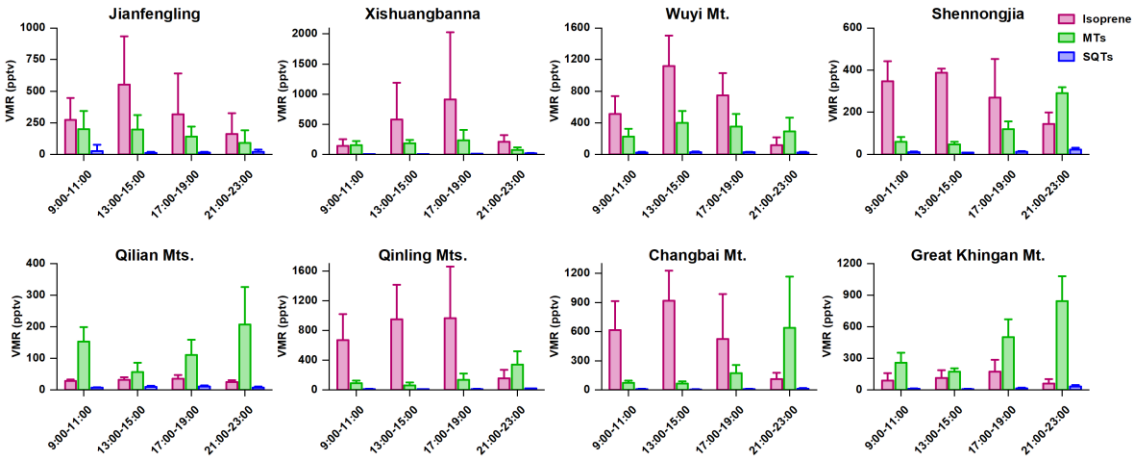


Figure S7. Diurnal patterns of BVOC mixing ratios in summer.

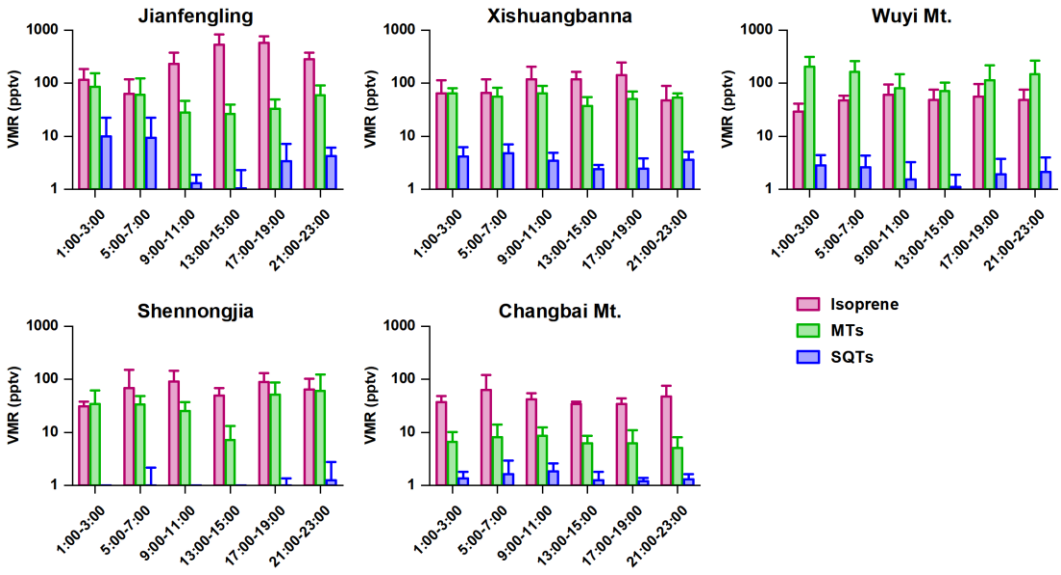


Figure S8. Diurnal patterns of BVOC mixing ratios in winter.

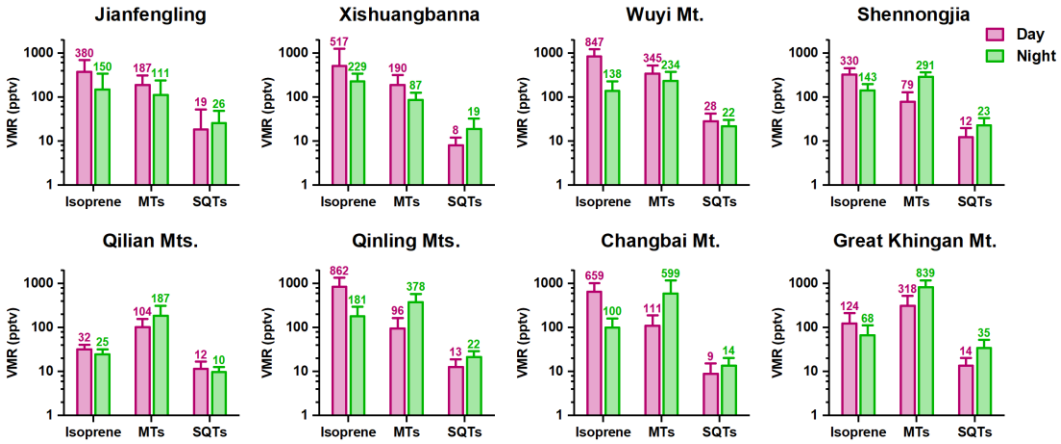


Figure S9. Daytime and nighttime averages of BVOC mixing ratios in summer.

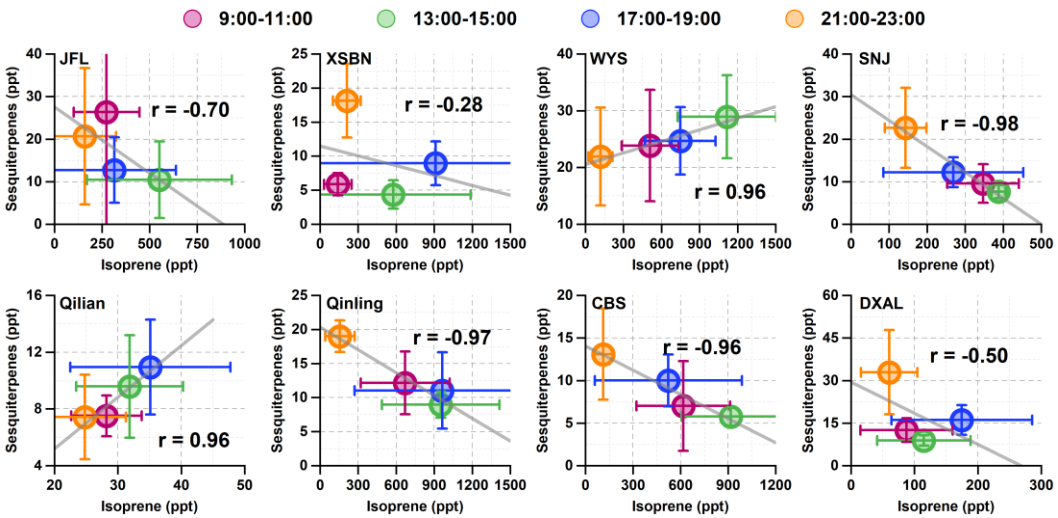


Figure S10. Correlation between isoprene and SQT mixing ratios at the four fixed summer sampling periods. Each point represents a sampling-period mean.

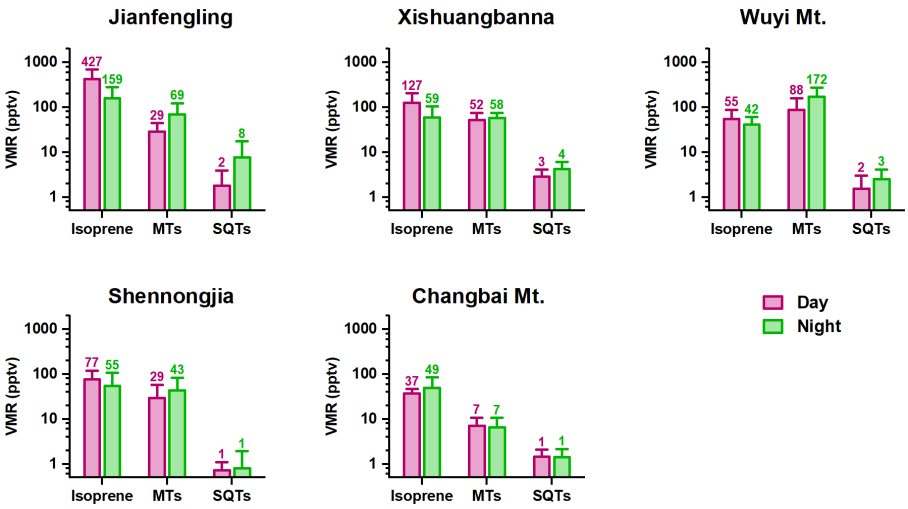


Figure S11. Daytime and nighttime averages of BVOC mixing ratios in winter.

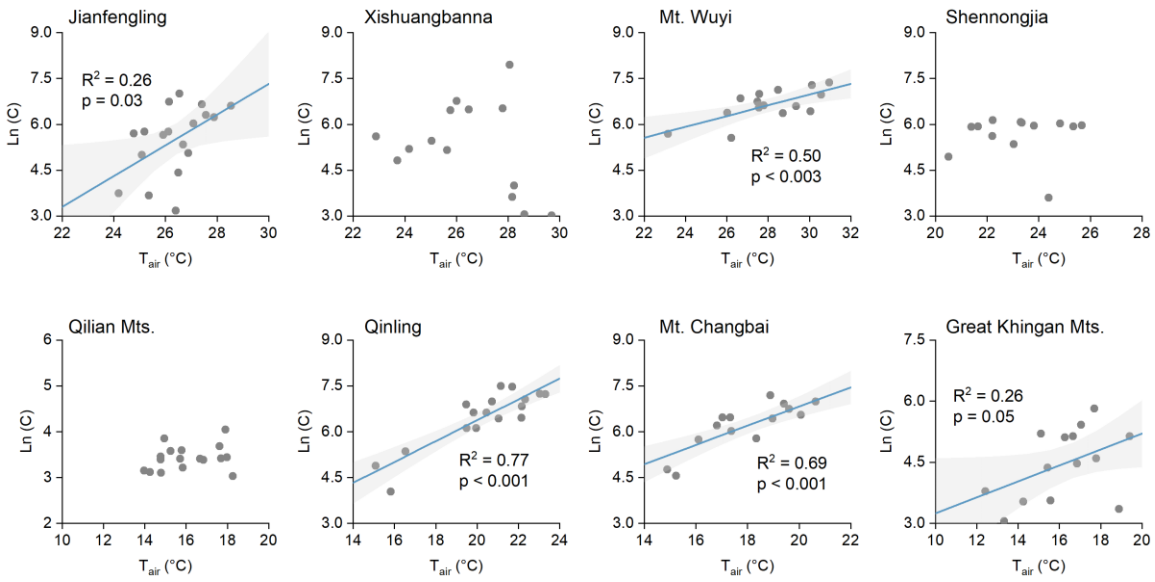


Figure S12. Correlation between daytime logarithmically transformed isoprene mixing ratios [ln(C)] and air temperature.

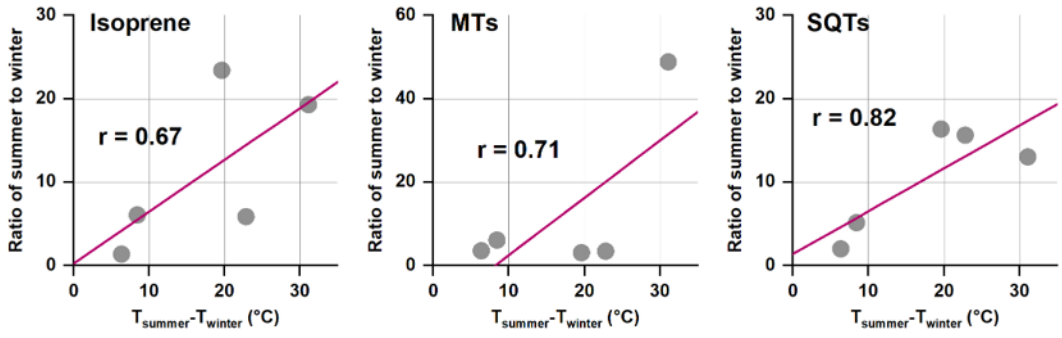


Figure S13. Correlation between the summer-to-winter ratio of BVOC mixing ratios and the summer-to-winter temperature difference (T_{summer} - T_{winter}) at the five sites sampled in both seasons.

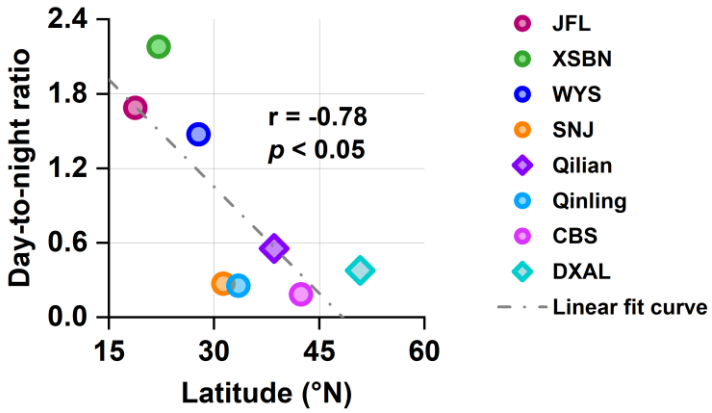


Figure S14. Relationship between latitude and the summer MT day-to-night mixing-ratio proxy across eight sites. The concentration ratio is not a direct measure of emission light dependence.

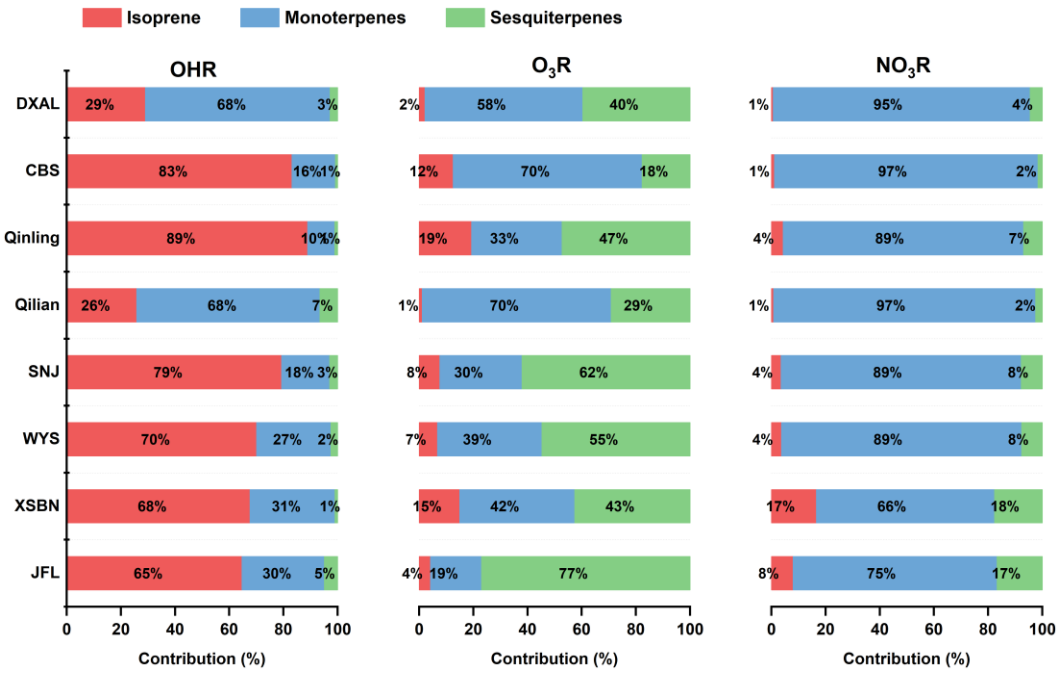


Figure S15. Calculated contribution of each BVOC class to OHR, O3R, and NO3R. The denominator is the summed reactivity of the measured BVOC species, not measured total ambient oxidant reactivity.

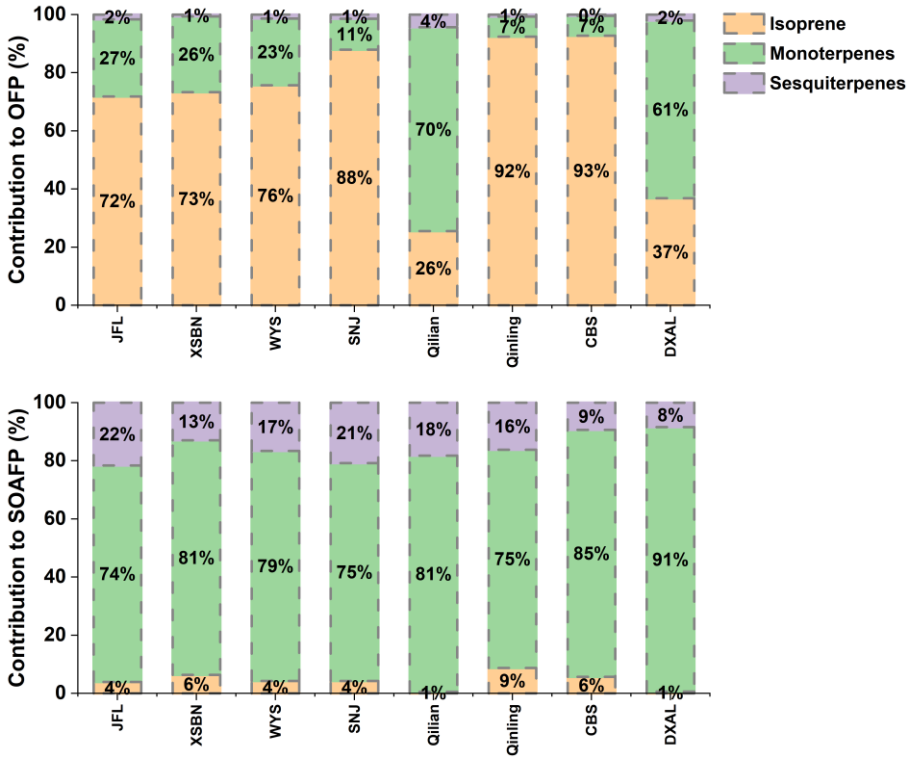


Figure S16. Calculated contribution of each BVOC class to OFP and SOAFP for the measured species. These are contributions to calculated potentials, not observed ozone or SOA formation.

Table S1. Site and sampling information for each forest.

Forest sites	Longitude (E)	Latitude (N)	Seasons	Sample No.	Temp. (°C)	Climate zone	Forest type
JFL	108.867	18.738	Summer	23	29.1	tropical	Broadleaf rainforest
			Winter	33	22.8		
XSBN	100.897	22.087	Summer	22	27.0	tropical	Broadleaf rainforest
			Winter	32	18.6		
WYS	117.691	27.747	Summer	21	32.5	subtropical	Broadleaf forest
			Winter	36	12.9		
SNJ	110.490	31.320	Summer	17	29.7	subtropical	Broadleaf forest
			Winter	34	6.9		
QL	108.448	33.434	Summer	23	26.2	subtropical to temperate	Broadleaf forest
			Winter	/	/		
QLS	100.290	38.568	Summer	23	24.4	temperate	Shrub and grass
			Winter	/	/		
CBS	128.107	42.399	Summer	21	19.0	temperate	Broadleaf forest
			Winter	33	-12.1		
DXAL	121.597	50.820	Summer	21	18.4	cold-temperate	Needleleaf forest
			Winter	/	/		

Table S2. Reaction rate constant of different BVOC with oxidants.

Compound	k_{O3} ($\times 10^{-17}$ cm^3 molecule^{-1} s^{-1})	k_{OH} ($\times 10^{-12}$ cm^3 molecule^{-1} s^{-1})	k_{NO3} ($\times 10^{-12}$ cm^3 molecule^{-1} s^{-1})
Isoprene	1.28	100	0.7
α-Pinene	8.7	53.7	6.1
Camphene	1.5	53	0.66
β-Pinene	1.9	78.9	2.5
β-Myrcene	47	210	11
3-Carene	4.9	87	9.1
α-Phellandren	290	313	73
α-terpinene*	8.7	53.7	6.1
Limonene	22	171	12
1.8-Cineole	0.015	11.1	0.00017
γ-Terpinene	14	177	29
Terpinolene	188	225	97
Linalool	43	159	11
α-Longipinene	43	96	9.26
Longicylene	1.14	47	0.68
β-Caryophyllene	1200	197	19
Thujopsene	43	93	8.97
Aromadendrene	1.2	62	5.98
Alloaromadendrene	1.2	62.5	6.03

Rate constants were compiled from Corchnoy & Atkinson (1990), Atkinson (1997), Hoffmann et al. (1997), Atkinson & Arey (2003), Bouvier-Brown et al. (2009a; 2009b), Hakola et al. (2012), Frazier et al. (2022), and IUPAC (http://iupac.pole-ether.fr). * For the tentatively assigned α-terpinene peak, α-pinene rate constants were assigned as surrogate values.

Table S3. MIR and SOA yield for different BVOC species.

Compound	MIR (ppb O_3/ppb BVOC)	SOA yield (%)
Isoprene	15.03	2
α-Pinene	12.78	32
Camphene	12.78	32
β-Pinene	9.97	31
β-Myrcene	11.45	43
3-Carene	9.18	38
α-Phellandren	11.45	0.84
α-terpinene	11.45	32
Limonene	12.89	58
1.8-Cineole	12.96	18
γ-Terpinene	11.45	25
Terpinolene	18.02	31
Linalool	12.96	13
α-Longipinene	7.27	65
Longicylene	7.27	65
β-Caryophyllene	7.27	68
Thujopsene	7.27	68
Aromadendrene	7.27	37
Alloaromadendrene	7.27	37

Values of MIR and SOA yield were compiled from Lee et al. (2006), Iinuma et al. (2008), Carter et al. (2010), and Mackenzie-Rae et al. (2017). The original unit (g O_3/g BVOC) of MIR were converted to ppb O_3/ppb BVOC in this study.

Table S4. Comparison of observed BVOC mixing ratios for different forest types.

Forest type	Site	Long.	Lat.	Year	Isoprene	MTs	SQTs	Notes	References
Tropical broadleaf rainforest	Jianfenglin, China	108.867	18.738	2019	332±299	172±147	20±38	Summer	This study
	Xishuangbanna, China	100.897	22.087	2019	434±641	164±124	12±10	Summer	This study
	INSTANT tower, Brazil	-59.000	-2.457	2012	9300±4900			Dry-to-wet transition	Gomes Alves et al., 2023
				2013	1010±660			Wet	
				2013	1840±1440			Wet	
				2013	1830±820			Dry-to-wet transition	
				2013	5020±1990			Dry	
				2014	5920±4890			Wet	
				2014	2920±2500			Wet	
				2014	7760±2490			Dry	
				2015	8940±1410			Dry-El Niño year	
	BR-Sa1 tower site, Brazil	-54.959	-2.857	2014	2700-4000	370-500			Sarkar et al., 2020
	ATTO site, Brazil	-59.000	-2.144	2015		910±100		12m, day	Yáñez-Serrano et al., 2018
						620±190		12m, night	
				2012-2014		820±340		24m, day	
						450±130		24m, night	
	Manacapuru rural site (T3), Brazil	-60.599	-3.213	2014			4.6		Yee et al., 2018
	Borneo, Malaysia	118.454	5.248	2008	13000	330		Oil palm forest	Misztal et al., 2011
	Bukit Atur Global Atmosphere Watch (GAW) station, Malaysia	117.844	4.98	2008	1058±889	285±265			Jones et al., 2011
Subtropical broadleaf forest	Mt. Wuyi, China	117.691	27.747	2019	639±469	329±199	27±13	Summer	This study
	Mt. Tian Jing, China	112.899	24.685	2016	287±32				Gong et al., 2018
	Mt. Tai Mo Shan, China	114.118	22.405	2010	109				Guo et al., 2012
Temperate broadleaf forest	Shengnongjia	110.490	31.320	2019	286±139	129±112	15±10	Summer	This study
	Qinling Mts., China	108.448	33.434	2019	709±540	150±150	15±8	Summer	This study
	Mt. Changbai, China	128.107	42.399	2019	503±412	261±371	11±7		This study
	Mt. Wudang, China	111.07	32.45	2018	210±300				Li et al., 2021
	Wytham Woods, UK	-1.339	51.773	2018	440			Top canopy	Otu-Larbi et al., 2020
					240			Middle canopy	
					170			Trunk level	
	Montseny site, Spain	2.358	41.779	2009	152-753	127-1421		Oak forest	Seco et al., 2011
	Mt. Tai, China	117.11	36.26	2006	173±174				Suthawaree et al., 2010

Table S4 (continue). Comparison of observed BVOC mixing ratios for different forest types.

Forest type	Site	Long.	Lat.	Year	Isoprene	MTs	SQTs	Notes	References
Temperate and boreal needleleaf forest	Great Khingan Mts., China	121.597	50.820	2019	106±84	470±356	19±14	Summer	This study
	Norunda research station, Sweden	17.483	60.083	2020	250	1000-1500	15-35		Petersen et al., 2025
	SMEAR II site, Finland	24.283	61.85	2011		398			Hellén et al., 2018
				2015		442			
				2016		427	13		
	Wakayama Forest, Japan	135.017	34.017	2014	595	709	27±8	Mean	Ramasamy et al., 2016
					835	622		Day	
					168	782		Night	
	MEFO, USA	-105.094	39.101	2011			0.7		Chan et al., 2016
	Taunus Observatory, Germany (Norway spruce)	8.433	50.217	2011		500±210	90±80	June	Bourtsoukidis et al., 2014
						410±180	100±70	July	
						560±370	100±60	August	
	Blodgett Forest, USA (Ponderosa pine)	120.63	38.9	2009		1100	95	Mean	Park et al., 2014
						600	72	Day	
						1300	98	Night	
	SMEAR II site, Finland	24.283	61.85	2010-2011		670	<3	Day	Hakola et al., 2012
						60	<3	Night	
	Blodgett Forest, USA (Ponderosa pine)	-120.63	38.9	2007		722	44.5	Day	Bouvier-Brown et al., 2009a
						2113	43.9	Night	
Grass/shrub land	Qilian Mts., China	100.290	38.568	2019	30±9	131±101	11±5	Summer	This study
	Maktau field site, Kenya	33.233	-3.417	2019	55.3±56	57.8±46			Liu et al., 2021
	Mt. Waliguan, China	100.9	36.28	2003	130				Xue et al., 2013

Table S5. Calculated OH reactivity from selected biogenic compounds in forest studies.

Forest type	Site	Long.	Lat.	Year	OH reactivity (s^{-1})	Note	References
Tropical broadleaf rainforest	ATTO site, Brazil	-59.000	-2.144	2018	10.41±4.21	March 2018, 80m; Isoprene + MTs + SQTs	Pfannerstill et al., 2021
				2018	15.57±7.86	October 2018, 80m; Isoprene + MTs + SQTs	
				2019	8.21±4.75	June 2019, 80m; Isoprene + MTs + SQTs	
				2019	14.52±7.46	September 2019, 80m; Isoprene + MTs + SQTs	
				2015	2.4	24m, MTs only	Yáñez-Serrano et al., 2018
				2015	3.4	12m, MTs only	
				2015	9.21±5.15	Isoprene only	Pfannerstill et al., 2018
				2012-2013	8.86	Dry season, 24m; Isoprene + MTs	Nölscher et al., 2016
					2.4	Wet season, 24m; Isoprene + MTs	
	Bukit Atur Global Atmosphere Watch (GAW) station, Malaysia	117.844	4.98	2008	3.27	Isoprene + MTs	Jones et al., 2011
Temperate broadleaf/ mixed forest	Talladega National Forest, USA	-87.13	32.95	2013	12.3	Isoprene + MTs	Heald et al., 2020
	Oak observatory, France	5.712	55.932	2014	24.1	Isoprene only, 20m	Zannoni et al., 2016
				2014	14.8	Isoprene only, 10m	
	University of Michigan Biological Station, USA	-84.7	45.5	2000	~3.5	at ~25 °C; Isoprene + MTs	Di Carlo et al., 2004
Temperate and boreal needleleaf forest	Taehwa Research Forest, Korea	127.319	37.305	2015	~2	Isoprene + MTs	Sanchez et al., 2021
	SMEAR II site, Finland	24.283	61.85	2015	1.6	all BVOCs	Hellen et al., 2018
	Manitou Forest Observatory, USA	-105.094	39.101	2011	4.43	Isoprene + MTs + MBO	Hunter et al., 2017
	Wakayama Forest Research Station, Japan	135.017	34.017	2014	3.43	Isoprene + MTs + SQTs	Ramasamy et al., 2016
	Manitou Forest Observatory, USA	-105.094	39.101	2008	3.1	Isoprene + MTs + SQTs + MBO	Nakashima et al., 2014
	SMEAR II site, Finland	24.283	61.85	2008	1.5	Isoprene + MTs	Sinha et al., 2010

Table S6. Observed total OH reactivity at different forest sites.

Forest type	Site	Long.	Lat.	Year	OH reactivity (s^{-1})	Note	References
Tropical broadleaf rainforest	ATTO site, Brazil	-59.000	-2.144	2018	23.70±6.52	March 2018, 80m	Pfannerstill et al., 2021
				2018	28.05±7.92	October 2018, 80m	
				2019	19.85±6.15	June 2019, 80m	
				2019	29.13±10.78	September 2019, 80m	
				2015	26.8	2015	Pfannerstill et al., 2018
				2012	28.1	2012	
				2012	11.0±11.7	November 2012, 0.05m	Nölscher et al., 2016
				2012	20.7±16.8	November 2012, 24m	
				2012	19.6±14.2	November 2012, 79.3m	
				2013	7.4±4.7	March 2013, 0.05m	
				2013	9.9±5.2	March 2013, 24m	
				2013	11.3±6.5	March 2013, 79.3m	
				2013	21.2±9.3	June 2013, 0.05m	
				2013	26.1±13.8	June 2013, 24m	
				2013	31.4±15.4	June 2013, 79.3m	
				2013	38.4±28.3	September 2013, 0.05m	
				2013	62.4±41.3	September 2013, 24m	
				2013	60.2±37.8	September 2013, 79.3m	
	GAW station, Malaysia	117.844	4.98	2008	20.3±10.1	Day	Edwards et al., 2013
				2008	9.6±3.0	Night	
Temperate broadleaf/ mixed forest	Talladega National Forest, USA	-87.13	32.95	2013	19.3		Heald et al., 2020
	Oak observatory, France	5.712	55.932	2014	29	2m, Oak forest	Zannoni et al., 2016
				2014	20	10m, Oak forest	
	University of Michigan Biological Station, USA	-84.7	45.5	2000	~12	At ~25 °C	Di Carlo et al., 2004
Temperate and boreal needleleaf forest	Taehwa Research Forest, Korea	127.319	37.305	2015	16.5		Sanchez et al., 2021
	Wakayama Forest Research Station, Japan	135.017	34.017	2014	7.1±3.4		Ramasamy et al., 2016
	Manitou Forest Observatory, USA	-105.094	39.101	2008	6.7		Nakashima et al., 2014
				2010	6	Day	Kim et al., 2013
				2010	10	Night	
	SMEAR II site, Finland	24.283	61.85	2010	12.4±0.1	Within canopy	Nölscher et al., 2012
				2010	11.5±0.1	Above canopy	
				2008	9		Sinha et al., 2010

References

Corchnoy, S. B., & Atkinson, R. (1990). Kinetics of the gas-phase reactions of OH and NO 3 radicals with 2-Carene, 1,8-Cineole, p-Cymene, and Terpinolene. Environmental Science & Technology, 24, 1497-1502.

Atkinson, R. (1997). Gas-phase tropospheric chemistry of volatile organic compounds: 1. Alkanes and alkenes. J. Phys. Chem. Ref. Data, 26, 215-290.

Hoffmann, T., Odum, J. R., Bowman, F., Collins, D., Klockow, D., Flagan, R. C., & Seinfeld, J. H. (1997). Formation of organic aerosols from the oxidation of biogenic hydrocarbons. J. Atmos. Chem., 26, 189-222.

Atkinson, R., & Arey, J. (2003). Atmospheric degradation of volatile organic compounds. Chemical Reviews, 103, 4605-4638.

Bouvier-Brown, N. C., Goldstein, A. H., Gilman, J. B., Kuster, W. C., & de Gouw, J. A. (2009a). In-situ ambient quantification of monoterpenes, sesquiterpenes, and related oxygenated compounds during BEARPEX 2007: implications for gas- and particle-phase chemistry. Atmospheric Chemistry and Physics, 9, 5505-5518.

Bouvier-Brown, N. C., Holzinger, R., Palitzsch, K., & Goldstein, A. H. (2009b). Large emissions of sesquiterpenes and methyl chavicol quantified from branch enclosure measurements. Atmospheric Environment, 43, 389-401.

Hakola, H., Hellén, H., Hemmilä, M., Rinne, J., & Kulmala, M. (2012). In situ measurements of volatile organic compounds in a boreal forest. Atmospheric Chemistry and Physics, 12, 11665-11678.

Frazier, G., McGlynn, D. F., Barry, L., Lerdau, M., Pusede, S. E., & Isaacman-VanWertz, G. (2022). Composition, Concentration, and Oxidant Reactivity of Sesquiterpenes in the Southeastern U.S. Environmental Science: Atmospheres, 2, 1208.

Lee, A., Goldstein, A. H., Kroll, J. H., Ng, N. L., Varutbangkul, V., Flagan, R. C., & Seinfeld, J. H. (2006). Gas-phase products and secondary aerosol yields from the photooxidation of 16 different terpenes. Journal of Geophysical Research: Atmospheres, 111, D17305.

Carter WPJCARBC. Updated maximum incremental reactivity scale and hydrocarbon bin reactivities for regulatory applications. 2009; 339: 2009.

Mackenzie-Rae, F. A., Liu, T., Deng, W., Saunders, S. M., Fang, Z., Zhang, Y., and Wang, X.: Ozonolysis of α-phellandrene - Part 1: Gas- and particle-phase characterization. Atmospheric Chemistry and Physics, 17, 6583-6609.

Gomes Alves, E., Aquino Santana, R., Quaresma Dias-Júnior, C., Botía, S., Taylor, T., Yáñez-Serrano, A. M., et al. (2023). Intra- and interannual changes in isoprene emission from central Amazonia. Atmospheric Chemistry and Physics, 23, 8149-8168.

Sarkar, C., Guenther, A. B., Park, J.-H., Seco, R., Alves, E., Batalha, S., et al. (2020). PTR-TOF-MS eddy covariance measurements of isoprene and monoterpene fluxes from an eastern Amazonian rainforest. Atmospheric Chemistry and Physics, 20, 7179-7191.

Yáñez-Serrano, A. M., Nölscher, A. C., Bourtsoukidis, E., Gomes Alves, E., Ganzeveld, L., Bonn, B., et al. (2018). Monoterpene chemical speciation in a tropical rainforest: variation with season, height, and time of day at the Amazon Tall Tower Observatory (ATTO). Atmospheric Chemistry and Physics, 18, 3403-3418.

Yee, L. D., Isaacman-VanWertz, G., Wernis, R. A., Meng, M., Rivera, V., Kreisberg, N. M., et al. (2018). Observations of sesquiterpenes and their oxidation products in central Amazonia during the wet and dry seasons. Atmospheric Chemistry and Physics, 18, 10433-10457.

Misztal, P. K., Nemitz, E., Langford, B., Di Marco, C. F., Phillips, G. J., Hewitt, C. N., et al. (2011). Direct ecosystem fluxes of volatile organic compounds from oil palms in South-East Asia. Atmos. Chem. Phys., 11, 8995-9017.

Jones, C. E., Hopkins, J. R., & Lewis, A. C. (2011). In situ measurements of isoprene and monoterpenes within a south-east Asian tropical rainforest. Atmospheric Chemistry and Physics, 11, 6971-6984.

Gong, D., Wang, H., Zhang, S., Wang, Y., Liu, S. C., Guo, H., et al. (2018). Low-level summertime isoprene observed at a forested mountaintop site in southern China: implications for strong regional atmospheric oxidative capacity. Atmospheric Chemistry and Physics, 18, 14417-14432.

Guo, H., Ling, Z. H., Simpson, I. J., Blake, D. R., & Wang, D. W. (2012). Observations of isoprene, methacrolein (MAC) and methyl vinyl ketone (MVK) at a mountain site in Hong Kong. Journal of Geophysical Research: Atmospheres, 117, D19303.

Li, Y., Gao, R., Xue, L., Wu, Z., Yang, X., Gao, J., et al. (2021). Ambient volatile organic compounds at Wudang Mountain in Central China: Characteristics, sources and implications to ozone formation. Atmospheric Research, 250, 105359.

Otu-Larbi, F., Bolas, C. G., Ferracci, V., Staniaszek, Z., Jones, R. L., Malhi, Y., et al. (2020). Modelling the effect of the 2018 summer heatwave and drought on isoprene emissions in a UK woodland. Glob Chang Biol, 26, 2320-2335.

Seco, R., Peñuelas, J., Filella, I., Llusià, J., Molowny-Horas, R., Schallhart, S., et al. (2011). Contrasting winter and summer VOC mixing ratios at a forest site in the Western Mediterranean Basin: the effect of local biogenic emissions. Atmos. Chem. Phys., 11, 13161-13179.

Suthawaree, J., Kato, S., Okuzawa, K., Kanaya, Y., Pochanart, P., Akimoto, H., et al. (2010). Measurements of volatile organic compounds in the middle of Central East China during Mount Tai Experiment 2006 (MTX2006): observation of regional background and impact of biomass burning. Atmos. Chem. Phys., 10, 1269-1285.

Petersen, R. C., Holst, T., Wu, C., Krejci, R., Chan, J. K., Mohr, C., & Rinne, J. (2025). BVOC and speciated monoterpene concentrations and fluxes at a Scandinavian boreal forest. Atmospheric Chemistry and Physics, 25, 17205-17236.

Hellén, H., Praplan, A. P., Tykka, T., Ylivinkka, I., Vakkari, V., Back, J., et al. (2018). Long-term measurements of volatile organic compounds highlight the importance of sesquiterpenes for the atmospheric chemistry of a boreal forest. Atmospheric Chemistry and Physics, 18, 13839-13863.

Ramasamy, S., Ida, A., Jones, C., Kato, S., Tsurumaru, H., Kishimoto, I., et al. (2016). Total OH reactivity measurement in a BVOC dominated temperate forest during a summer campaign, 2014. Atmospheric Environment, 131, 41-54.

Chan, A. W. H., Kreisberg, N. M., Hohaus, T., Campuzano-Jost, P., Zhao, Y., Day, D. A., et al. (2016). Speciated measurements of semivolatile and intermediate volatility organic compounds (S/IVOCs) in a pine forest during BEACHON-RoMBAS 2011. Atmospheric Chemistry and Physics, 16, 1187-1205.

Bourtsoukidis, E., Williams, J., Kesselmeier, J., Jacobi, S., & Bonn, B. (2014). From emissions to ambient mixing ratios: online seasonal field measurements of volatile organic compounds over a Norway spruce-dominated forest in central Germany. Atmospheric Chemistry and Physics, 14, 6495-6510.

Park, J. H., Fares, S., Weber, R., & Goldstein, A. H. (2014). Biogenic volatile organic compound emissions during BEARPEX 2009 measured by eddy covariance and flux-gradient similarity methods. Atmos. Chem. Phys., 14, 231-244.

Hakola, H., Hellén, H., Hemmilä, M., Rinne, J., & Kulmala, M. (2012). In situ measurements of volatile organic compounds in a boreal forest. Atmospheric Chemistry and Physics, 12, 11665-11678.

Liu, Y., Schallhart, S., Taipale, D., Tykkä, T., Räsänen, M., Merbold, L., et al. (2021). Seasonal and diurnal variations in biogenic volatile organic compounds in highland and lowland ecosystems in southern Kenya. Atmospheric Chemistry and Physics, 21, 14761-14787.

Xue, L. K., Wang, T., Guo, H., Blake, D. R., Tang, J., Zhang, X. C., et al. (2013). Sources and photochemistry of volatile organic compounds in the remote atmosphere of western China: results from the Mt. Waliguan Observatory. Atmos. Chem. Phys., 13, 8551-8567.

Pfannerstill, E. Y., Nölscher, A. C., Yáñez-Serrano, A. M., Bourtsoukidis, E., Keßel, S., Janssen, R. H. H., et al. (2018). Total OH reactivity changes over the Amazon rainforest during an El Niño event. Frontiers in Forests and Global Change, 1, 12.

Pfannerstill, E. Y., Reijrink, N. G., Edtbauer, A., Ringsdorf, A., Zannoni, N., Araújo, A., et al. (2021). Total OH reactivity over the Amazon rainforest: variability with temperature, wind, rain, altitude, time of day, season, and an overall budget closure. Atmospheric Chemistry and Physics, 21, 6231-6256.

Yáñez-Serrano, A. M., Nölscher, A. C., Bourtsoukidis, E., Gomes Alves, E., Ganzeveld, L., Bonn, B., et al. (2018). Monoterpene chemical speciation in a tropical rainforest: variation with season, height, and time of day at the Amazon Tall Tower Observatory (ATTO). Atmospheric Chemistry and Physics, 18, 3403-3418.

Nolscher, A. C., Yanez-Serrano, A. M., Wolff, S., de Araujo, A. C., Lavric, J. V., Kesselmeier, J., & Williams, J. (2016). Unexpected seasonality in quantity and composition of Amazon rainforest air reactivity. Nature Communications, 7, 10383.

Heald, C. L., Gouw, J., Goldstein, A. H., Guenther, A. B., Hayes, P. L., Hu, W., et al. (2020). Contrasting reactive organic carbon observations in the Southeast United States (SOAS) and Southern California. Environmental Science & Technology, 54, 14923-14935.

Zannoni, N., Gros, V., Lanza, M., Sarda, R., Bonsang, B., Kalogridis, C., et al. (2016). OH reactivity and concentrations of biogenic volatile organic compounds in a Mediterranean forest of downy oak trees. Atmospheric Chemistry and Physics, 16, 1619-1636.

Di Carlo, P., Brune, W. H., Martinez, M., Harder, H., Lesher, R., Ren, X. R., et al. (2004). Missing OH reactivity in a forest: Evidence for unknown reactive biogenic VOCs. Science, 304, 722-725.

Sanchez, D., Seco, R., Gu, D., Guenther, A., Mak, J., Lee, Y., et al. (2021). Contributions to OH reactivity from unexplored volatile organic compounds measured by PTR-ToF-MS - a case study in a suburban forest of the Seoul metropolitan area during the Korea-United States Air Quality Study (KORUS-AQ) 2016. Atmospheric Chemistry and Physics, 21, 6331-6345.

Hunter, J. F., Day, D. A., Palm, B. B., Yatavelli, R. L. N., Chan, A. W. H., Kaser, L., et al. (2017). Comprehensive characterization of atmospheric organic carbon at a forested site. Nature Geoscience, 10, 748-753.

Nakashima, Y., Kato, S., Greenberg, J., Harley, P., Karl, T., Turnipseed, A., et al. (2014). Total OH reactivity measurements in ambient air in a southern Rocky mountain ponderosa pine forest during BEACHON-SRM08 summer campaign. Atmospheric Environment, 85, 1-8.

Sinha, V., Williams, J., Lelieveld, J., Ruuskanen, T. M., Kajos, M. K., Patokoski, J., et al. (2010). OH reactivity measurements within a boreal Forest: Evidence for unknown reactive emissions. Environmental Science & Technology, 44, 6614-6620.

Edwards, P. M., Aikin, K. C., Dube, W. P., Fry, J. L., Gilman, J. B., de Gouw, J. A., et al. (2017). Transition from high- to low-NO_x control of night-time oxidation in the southeastern US. Nature Geoscience, 10, 490-495.

Kim, S., Wolfe, G. M., Mauldin, L., Cantrell, C., Guenther, A., Karl, T., et al. (2013). Evaluation of HO_x sources and cycling using measurement-constrained model calculations in a 2-methyl-3-butene-2-ol (MBO) and monoterpene (MT) dominated ecosystem. Atmospheric Chemistry and Physics, 13, 2031-2044.